

Appendix 1: Site partitioning according to their climatic conditions.

The sites were assigned to one of two categories depending on whether they belong to oceanic or mediterranean climatic regions (hereafter called “soft-climate” sites, Figure 2A, red dots) or to semi-continental regions^{5 1} (hereafter called “harsh-climate” sites, Figure 2A, blue dots). To evaluate the relevance of this partitioning, we ran a discriminant analysis (ade4 package^{5 2}) from daily average temperatures estimated each day at each site using the SAFRAN spatially explicit database (8 x 8 km mesh size grid)^{5 3} during the 60-year period (1960 - 2020). For each site and each year, we calculated the annual average temperature and the temperature amplitude between the warmest and coldest month. From the time series of these two variables, between 1960 and 2020, we determined for each one the mean and standard deviation that will allow us to characterize whether the sites have soft climatic conditions (high mean annual temperature, low annual thermal amplitude, low variation in mean annual temperature and thermal amplitude between years) or harsh (reverse conditions). The discriminant analysis allows to find a linear combination of the 4 variables so that the coordinates of sites on the discriminant axis maximize the Mahalanobis distance^{5 4} between the two previously defined groups.

Note that the discrimination is perfect since all harsh sites are on the left of the origin and all soft sites on the right (Figure A1). The harsh sites are then characterized, as compared to the soft sites, by a lower annual temperature (Figure A1A), a higher inter-annual variability of annual temperature (Figure A1B), a higher annual amplitude of temperature (Figure A1C) and a higher inter-annual variability of annual amplitude of temperature (Figure A1D). To check the significance of our typology we use a permutation test : we assign randomly the sites to the soft or harsh group and repeat 10 000 times the discriminant analysis to generate the empirical distribution of the Mahalanobis distance between the two groups under the assumption of no significant difference in climate typology between groups of sites. The Mahalanobis distance observed from our initial typology (soft climate sites vs. harsh climate sites) is significantly smaller than those expected under H_0 (p-value= 0.01) confirming the robustness of the typology initially proposed.

Appendix 2: Statistics to characterize inter-annual variability in oak reproduction

Works dealing with masting have mobilized several statistics to describe interannual variability in fruit production dynamics, the mostly used being the coefficient of variation (CV = the standard deviation to mean ratio). One alternative measure, originally proposed by Heath⁵⁶ is the Proportional Variation (PV) that estimates the mean relative difference between all possible pairs of values in a time series; it is standardized (i.e., ranging from 0 to 1). While PVs overcomes some mathematical difficulties encountered by the CVs ⁶⁻⁸, this statistic has strong limitations. As it is saturating (maximum value equal to 1), it might be poorly efficient at discriminating between high levels of interannual variation in fruiting. Moreover, as it is based on the calculation of distances, it does not account for the difference between theoretical fruiting dynamics that would be radically different. For example, the same PVs values would be expected for (i) time series composed mainly of very low fruiting and including seldom years of massive fruiting and (ii) time series composed mainly of massive fruiting and seldom years of very low fruiting.

In this appendix, to overcome the problems with PV described above, we first ensured that PV and CV captured the same general information. Secondly, we examined the accuracy of the estimates of the level of interannual variability of reproduction with these two statistics. We therefore described the interannual variability of fruit production, flowering effort, and fruiting rate with these two statistics and examined their relationship. We then calculated their confidence intervals (CI) using a bootstrap analysis, as well as their relative confidence intervals (RCI = CI divided by the estimator) to compare the degree of accuracy of each estimator.

CVs and PVs were found to be highly correlated (Figure A3.1), which shows that the two statistics capture the same information about inter-annual variations in reproduction in this study. CI and RCI were very high for CVs , especially for population-level data (CV_p , Figure A3.1 et A3.2). In contrast, PV_p estimates were much more precise than their CV_p counterparts, displaying lower RCI regardless of the variable considered (Figure A3.2). The use of PVs therefore provides greater statistical power in the analysis of our results (see Figure A3.2 vs Figure 4, and table A5.2 vs table A5.1).

Given the ongoing debate about which statistics to use in the field of masting studies, and to allow the reader to compare the alternating results, we choose to present the results with the two statistics: (i) CVs in the main text, as it is the mostly used and easier to interpret biologically and (ii) PVs in the appendix because it is strongly correlated to CVs and confers greater statistical power in our study.

Figures

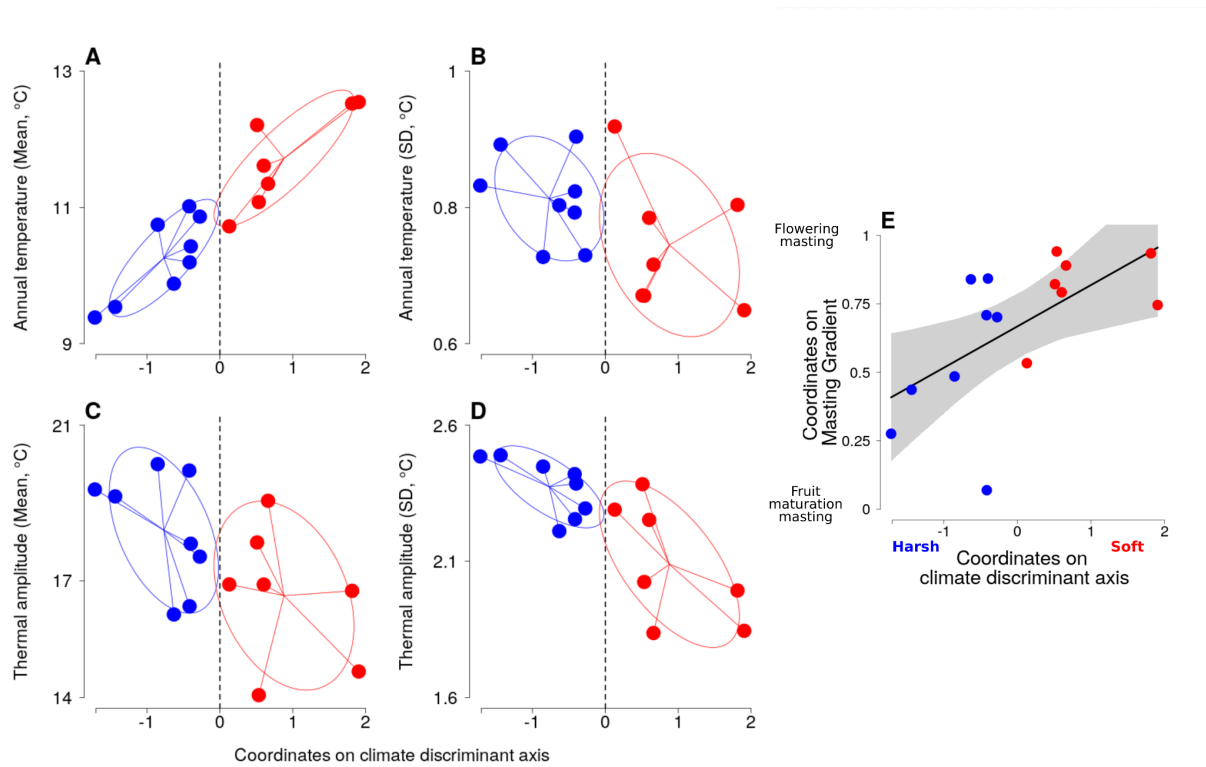


Figure S1 : Discriminant analysis between soft (red dots) and harsh (blue dots) climate sites and correlation between climate and masting gradients. The x -axis is the site coordinate on the discriminant axis. **A - D** : The y -axis is one of the four synthetic weather variables used, calculated over the period 1960-2020: **A** and **B** the mean and standard deviation of the annual mean temperature; **C** and **D** the mean and standard deviation of the annual temperature amplitude (difference between the mean of the temperatures of the warmest and coldest months). **E** : The y -axis is the coordinates of each site on the Fruit Maturation - Flowering Masting gradient described on Figure 2B-C. This gradient goes from 0 to 1 with sites at the zero-end having a fruit production dynamic governed exclusively by fruiting rate while those at the one-end are only driven by flowering dynamic. The full line represents the linear correlation between the y and x variables. Shaded area marks the 95% confidence interval around the model. This figure is related to Figure 2.

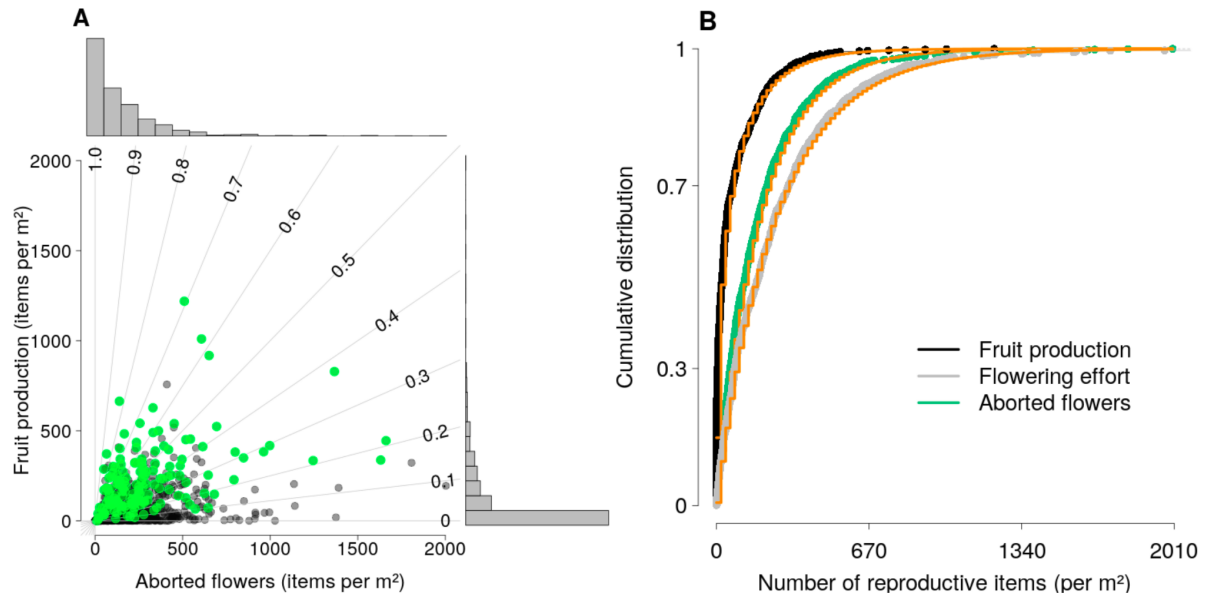


Figure S2 : Distribution of fruit production, aborted flowers and flowering effort. A : Number of fruits according to the number of aborted flowers produced each year by each tree (count per m² sampling surface). Fine lines delimit the graph according to fruiting rates whose values are shown on the graph. Green dots correspond to the maximum number of fruits produced by each tree over the 8-year survey. **B :** Cumulative distribution of the number of acorns (black dots), flowers (grey dots) and aborted flowers (green dots) counted per square meter. Orange lines represent the negative binomial distribution that best fits our data, based on AIC criterion (by comparison with normal, poisson, negative binomial and zero inflated negative binomial distributions, from the r package `fitdistrplus`⁵). This figure is related to Figure 1.

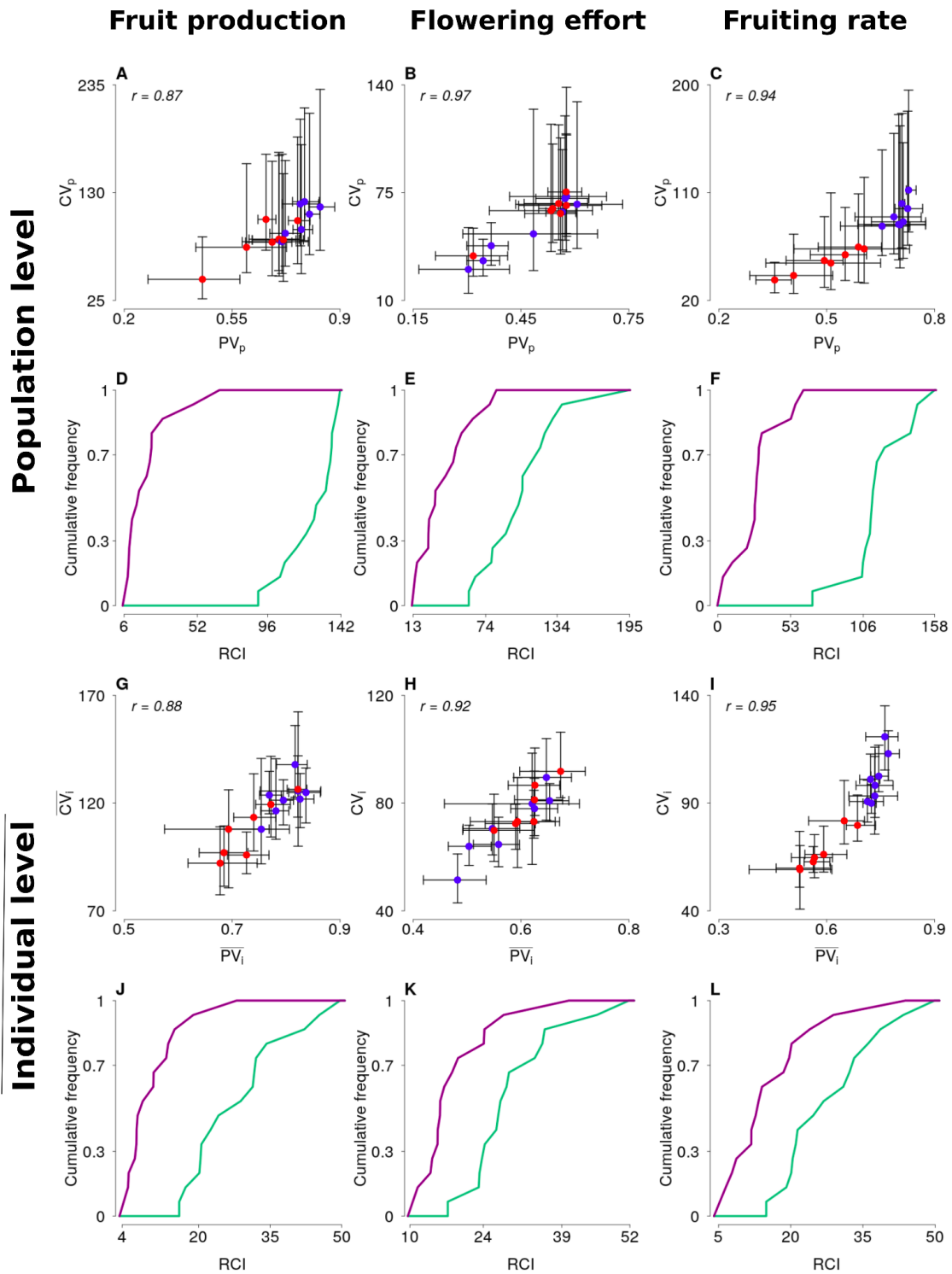


Figure S3: Relationships between PV and CV statistics describing interannual variation in oak reproduction and distribution of their Relative Confidence Intervals (RCI). A-F : interannual variation at the population level (CV_p and PV_p). G-L : averaged interannual individual variation (\overline{CV}_i and \overline{PV}_i). First column corresponds to estimators computed on fruit production while the second and the third are computed on flowering effort and fruiting rate, respectively. Red and blue dots on the first and third rows correspond to estimators at soft and hard climate sites, respectively. CIs are

obtained from bootstrapping (see method). The R coefficients indicated on those panels correspond to the orthogonal correlation coefficients between the two statistics. The purple curve on the second and fourth rows corresponds to PVs and the green curve to CVs . This figure is related to Figure 4.

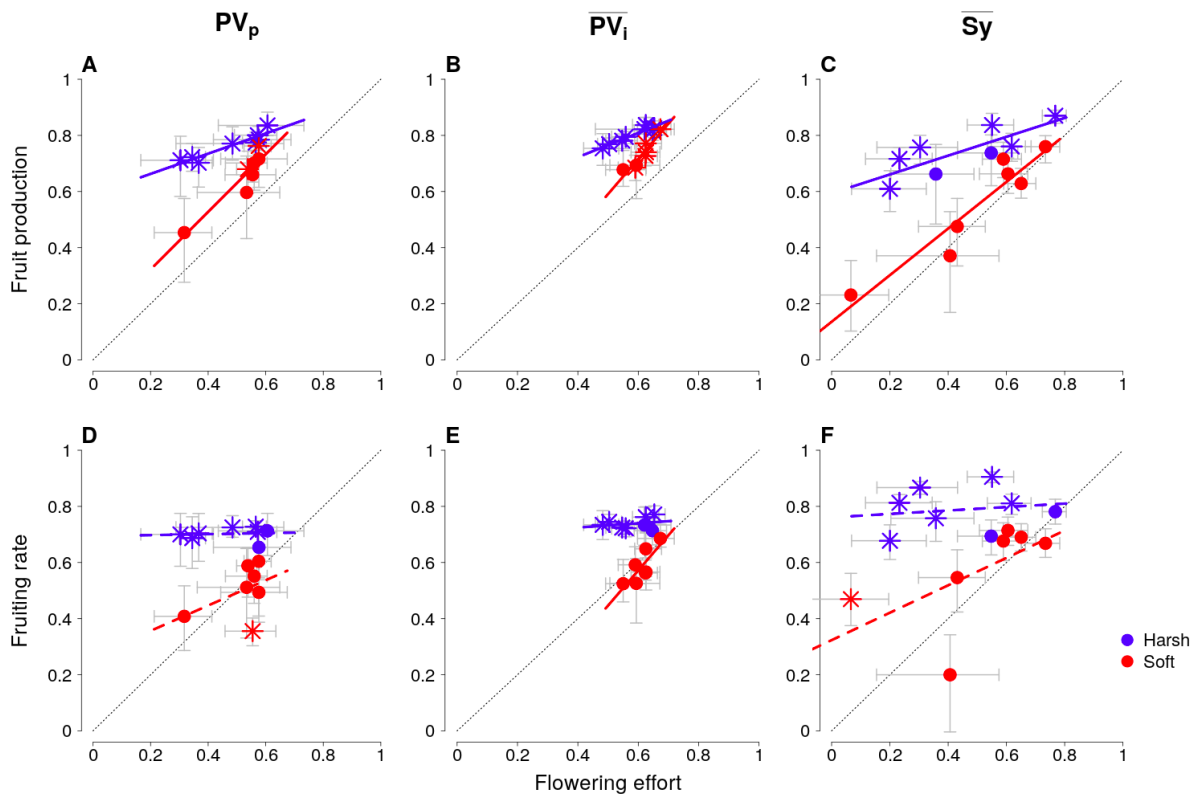


Figure S4 : Relationship between masting statistics applied to fruit production and flowering effort (A,B,C) and to fruiting rate and flowering effort (D,E,F). This figure mirrors Figure 4 when using coefficient of variation (PV) to account for interannual variability in flowering effort, fruit production and fruiting rate. First column (A,D) represents variability at population level (PV_p) while the second one uses statistics computed at individual-level (B,E)(\overline{PV}_i). The third column illustrates the degree of synchrony between individuals (\overline{S}_y , C and F). Error bars are the 95% confidence intervals of the statistics computed by means of bootstrapping method. Black dotted lines correspond to the first bisector ($y = x$). see legend of figure 4 for details on points and lines shape. This figure is related to Figure 4.

Tables

		Estimate	Std.Error	t value	Pr (> t)
Figure 1A	Intercept	-10.199	4.075	-2.503	0.013
	Slope	0.313	0.0008	37.171	< 2e-16
Figure 1B	Intercept	-20.668	7.5	-2.756	0.008
	Slope	0.359	0.0231	15.534	< 2e-16

Table S1 : Mean relationship between fruit production and flowering effort at individual and population level. Summary of Linear Mixed Models with fruit production (resp. mean fruit production) as dependent variable and individual tree (Figure 1A) (resp. population (Figure 1B)) as a random effect. Model linked to Figure 1A includes flowering effort as explanatory variables while the model linked to Figure 1B includes mean flowering effort at population scale. Significant p values are in bold.

		Climatic group	Estimate	Std.Error	Z value	Pr (> z)
Figure 3A	Intercept	Harsh	-6.713	0.113	8.094	5.77E-16
		Soft	-5.387	0.277		
	Slope	Harsh	0.506	0.003	-22.418	< 2e-16
		Soft	0.42	0.007		
Figure 3B	Intercept	Harsh	-5.483	0.105	24.91	< 2e-16
		Soft	-1.66	0.258		
	Slope	Harsh	0.403	0.001	-214.72	< 2e-16
		Soft	0.075	0.003		

Table S2 : Response of fruiting rate to flowering effort and mean april temperatures. Summary of Generalized Linear Mixed Models (GLMMs with binomial family) with fruiting rate as dependent variable and population as random effect. Model linked to Figure 3A includes flowering effort (with a $\log(1 + x)$ transformation), climatic group and their interaction as explanatory variables while the model linked to Figure 3B includes mean April's temperature, climatic group and their interaction. Test results for slope and intercept differences between climatic groups are given for each figure. Significant p values are in bold.

		Climatic group	Estimate	Std.Error	t	p value	R ²
Figure 4A	Intercept	Harsh	64,382	12,183	-3,072	0,0106	0,801
		Soft	-10,906	36,692			
	Slope	Harsh	0,697	0,216	1,996	0,0713	
		Soft	1,49	0,614			
Figure 4B	Intercept	Harsh	79,296	12,539	-3,333	0,0067	0,86
		Soft	-2,382	37,046			
	Slope	Harsh	0,596	0,171	2,536	0,0277	
		Soft	1,402	0,489			
Figure 4C	Intercept	Harsh	0,594	0,056	-5,552	0,0002	0,901
		Soft	0,136	0,138			
	Slope	Harsh	0,336	0,115	3,078	0,0105	
		Soft	0,831	0,276			
Figure 4D	Intercept	Harsh	81,31	12,923	-2,139	0,0557	0,829
		Soft	25,692	38,919			
	Slope	Harsh	0,192	0,23	0,558	0,588	
		Soft	0,427	0,651			
Figure 4E	Intercept	Harsh	98,042	22,808	-2,03	0,0672	0,802
		Soft	7,533	67,384			
	Slope	Harsh	0,043	0,312	1,255	0,2355	
		Soft	0,769	0,889			
Figure 4F	Intercept	Harsh	0,761	0,114	-2,593	0,025	0,594
		Soft	0,323	0,283			
	Slope	Harsh	0,061	0,235	1,297	0,2211	
		Soft	0,488	0,564			

Table S3 : Estimated parameters of the relationship between masting statistics. Masting statistics were applied to fruit production and flowering effort (Figure 4A to C) and to fruiting rate and flowering effort (Figure 4D to F). Each linear model includes the statistic computed on flowering effort, climatic group and their interaction. Test results for slope and intercept differences between climatic groups are given for each figure. Significant p values are in bold.

		Climatic Group	Estimate	Std.Error	t	p value	R ²
Figure A3.2A	Intercept	Harsh	0,591	0,048	-5,433	0,0002	0,913
		Soft	0,117	0,135			
	Slope	Harsh	0,36	0,097	3,946	0,0023	
		Soft	1,026	0,266			
Figure A3.2B	Intercept	Harsh	0,549	0,055	-4,9	0,0005	0,927
		Soft	-0,036	0,174			
	Slope	Harsh	0,433	0,094	4,166	0,0016	
		Soft	1,254	0,291			
Figure A3.2D	Intercept	Harsh	0,694	0,097	-2,402	0,0351	0,784
		Soft	0,266	0,275			
	Slope	Harsh	0,018	0,198	1,258	0,2343	
		Soft	0,451	0,542			
Figure A3.2E	Intercept	Harsh	0,694	0,105	-3,81	0,0029	0,902
		Soft	-0,18	0,334			
	Slope	Harsh	0,076	0,18	3,11	0,0099	
		Soft	1,253	0,559			

Table S4 : Estimated parameters of the relationship between *PV* statistics for masting. As we did for *CV* and *Sy* statistics, we computed *PV* statistics on fruit production and flowering effort (Figure A3.2A to A3.2C) and to fruiting rate and flowering effort (Figure A3.2D to A3.2F). Similar to Table A5.1 and Figure 4, we applied a linear model for each panel, models include the statistic computed on flowering effort, climatic group and their interaction. Test results for slope and intercept differences between climatic groups are given for figures A3.2A, B, D and E. See Table A5.1 for results associated with Figures A3.2C and F (respectively identical to Figures 4C and F). Significant p values are in bold.

Supplemental References

1. Météo-France (2020). Le climat en France métropolitaine. <https://meteofrance.com/comprendre-climat/france/le-climat-en-france-metropolitaine>.
2. Chessel, D., Dufour, A.-B., and Thioulouse, J. (2004). The ade4 Package – I: One-Table Methods. *R News* 4, 5–10.
3. Durand, Y., Brun, E., Merindol, L., Guyomarc'h, G., Lesaffre, B., and Martin, E. (1993). A meteorological estimation of relevant parameters for snow models. *Ann. Glaciol.* 18, 65–71. 10.3189/S0260305500011277.
4. Mahalanobis, P.C. (1936). On the Generalized Distance in Statistics. *Natl Inst Sci India*, 49–55.
5. Delignette-Muller, M.L., and Dutang, C. (2015). fitdistrplus : An R Package for Fitting Distributions. *J. Stat. Soft.* 64, 1–34. 10.18637/jss.v064.i04.
6. Heath, J.P. (2006). Quantifying temporal variability in population abundances. *Oikos* 115, 573–581. 10.1111/j.2006.0030-1299.15067.x.
7. Heath, J.P., and Borowski, P. (2013). Quantifying Proportional Variability. *PLoS ONE* 8, e84074. 10.1371/journal.pone.0084074.
8. Fernández-Martínez, M., Vicca, S., Janssens, I.A., Carnicer, J., Martín-Vide, J., and Peñuelas, J. (2018). The consecutive disparity index, D : a measure of temporal variability in ecological studies. *Ecosphere* 9, e02527. 10.1002/ecs2.2527.